



Photoelectrochemical Bisphenol S Sensor Based on ZnO-Nanorods Modified by Molecularly Imprinted Polypyrrole

Roman Viter,* Kwanele Kunene, Povilas Genys, Daniels Jevdokimovs, Donats Erts,*
Andris Sutka, Krishna Bisetty, Arturs Viksna, Almira Ramanaviciene,
and Arunas Ramanavicius*

Molecularly imprinted polymers are important tools for the design of sensors and other molecular recognition based analytical systems. In this paper the development of a photoelectrochemical sensor for selective bisphenol determination is reported. The sensor is based on a glass/ZnO/MIP-Ppy structure consisting of glass modified by a ZnO layer (glass/ZnO), which is functionalized by molecularly imprinted conducting polymer polypyrrole (MIP-Ppy). The sensitivity of the sensor to bisphenol is in the range of 0.7–12.5 μM . Selectivity tests to other bisphenolic compounds are performed. Some aspects of a photoinduced response mechanism in glass/ZnO/MIP-Ppy nanostructures are predicted and discussed.

1. Introduction

1 Dimensional semiconductor nanostructures are very efficient platforms for various sensing and biosensing applications due to high surface-to-volume ratio. Among different semiconductor nanostructures, 1D Zinc Oxide nanostructures have been widely used in different types of sensors due to their advanced electronic and optical properties.^[1] Some papers have been reported on the development of electrochemical^[2] and optical^[3] sensors and biosensors, based on 1D ZnO nanostructures.

1D ZnO nanostructures can be formed by different methods, such as chemical vapor deposition (CVD), thermal evaporation, pulsed laser deposition, etc.^[4] However, these techniques are costly and complex comparing to hydrothermal growth method. The hydrothermal method has a number of advantages, such as inexpensive simple deposition route at low temperature with high growth rate at environmentally friendly conditions. Moreover, hydrothermal method enables large-scale production of ZnO-based nanostructures with different morphology such as nanoflowers, nanoneedles, nanocups, nanopetals, and powders.^[5]

Bare ZnO surface might interact with a number of species that decrease a selectivity of sensor. To improve selectivity, the surface of ZnO nanostructures can be effectively functionalized by different groups, which are suitable for covalent binding of biomolecules.^[1,3] Moreover, ZnO nanostructures are compatible with other organic nanomaterials, such as conducting polymers (CP), therefore, nanocomposites based on ZnO and conducting polymers are used for sensor design.^[6–8]

Band-to-band transitions in semiconductors, induced by a light absorption, generate electron-hole pairs which participate in charge transfer.^[1,3] For instance, this effect can improve sensitivity of electrochemical sensors.^[1,3] ZnO is well known as wide bandgap semiconductor, which has band gap of 3.3 eV.^[1,3] Thus, UV light is required for the generation of photoelectrochemical response in ZnO-based electrochemical sensors.

Conducting polymers are optically active organic materials with tailored structural, electronic and optical properties. They have few absorption bands in the range of 310–325 nm, 420–470 nm, and 540–660 nm.^[9] Due to their molecular structure, CPs are used in gas, optical and electrochemical sensors devoted for selective detection of target molecules.

Dr. R. Viter, Dr. D. Jevdokimovs, D. Erts, Prof. A. Sutka
Institute of Chemical Physics, and Institute of Atomic Physics and Spectroscopy

University of Latvia
19 Raina Boulevard, LV 1586 Riga, Latvia
E-mail: roman.viter@lu.lv; donats.erts@lu.lv

K. Kunene, Prof. K. Bisetty
Department of Chemistry
Durban University of Technology
P.O Box 1334, Durban 4000, South Africa

Dr. R. Viter
Sumy State University
Center for Collective Use of Scientific Equipment
31, Sanatornaya st., 40018 Sumy, Ukraine

P. Genys, Prof. A. Ramanaviciene, Prof. A. Ramanavicius
NanoTechnas – Center of Nanotechnology and Materials Science
Faculty of Chemistry and Geosciences
Vilnius University
Naugarduko 24, LT-03225 Vilnius, Lithuania
E-mail: arunas.Ramanavicius@chf.vu.lt

Prof. A. Sutka
Research Laboratory of Functional Materials Technologies
Faculty of Materials Science and Applied Chemistry
Riga Technical University
P. Valdena 3/7, 1048 Riga, Latvia

K. Kunene, D. Erts, Prof. A. Viksna
Faculty of Chemistry
University of Latvia
19 Raina Boulevard, LV 1586 Riga, Latvia

The ORCID identification number(s) for the author(s) of this article can be found under <https://doi.org/10.1002/macp.201900232>.

DOI: 10.1002/macp.201900232

Polypyrrole (Ppy), the one of conducting polymers, has been widely used for sensor applications. During the formation of Ppy layers can be modified by molecular imprints and in such way molecularly imprinted Ppy can be formed (MIP-Ppy),^[10–16] which contains molecularly imprinted sites, which are complementary and selective for imprinted target molecules. The most efficient formation of MIP-Ppy can be based on electrochemical polymerization of the pyrrole monomer in the presence of target molecules.^[9–16] Electrochemically imprinted sites can be formed by small molecular organics such as caffeine,^[10,11] theophiline,^[12,13] histamine,^[14] relatively large DNA fragments, which are forming DNA aptamers,^[15] and even by relatively large proteins with molecular weight of over 50 KDa.^[16] The selectivity and sensitivity of MIP-Ppy-based sensors can be significantly improved by electrochemically performed overoxidation of formed Ppy layer. Moreover, the sensitivity of MIP-Ppy can be enhanced by selection of the most optimal conductive supports, for example, the application of semiconducting/catalytic materials with high ratio of surface area to volume.

ZnO/CP-based nanocomposites have been investigated in the number of researches.^[17–19] Due to different types of conductivity in ZnO and conducting polymers, p-n junction between ZnO and conducting polymers has been reported.^[17–19] In ZnO/CP-based sensors conducting polymer based coating acts as analyte-selective layer and sometimes it serves as a protecting coating, which protects ZnO from some interfering materials, in addition CP-based layer slows-down chemical/electrochemical dissolution and degradation of ZnO-nanorods (Zn-NRs).^[17]

Phenolic compounds, such as bisphenol A and bisphenol S are widely used in petrochemical products and in wood preservatives, textiles, plastics, dyes, paper, herbicides, and pesticides.^[20,21] The most of these compounds are highly toxic and cause many health problems, due to ability to penetrate through oral, dermal, or respiratory tracts.^[22,23] A number of analytical techniques are available for the determination of bisphenol A and bisphenol S. They include spectrophotometry,^[24] gas chromatography,^[25] liquid chromatograph,^[26] and capillary electrophoresis.^[27] However, some of these techniques (e.g., spectrophotometry) are not sensitive and specific while some others (e.g., gas chromatography, liquid chromatography and capillary electrophoresis) are cumbersome and require time-consuming sample pre-treatment, expensive equipment and well-skilled personnel.^[28] Recently, significant efforts have been focused on the development of simple, sensitive, selective and effective analytical methods for the determination of bisphenols.^[29–31] Among newly developed analytical methods for the determination of bisphenols electrochemical enzyme-based biosensors are very promising for in situ determination of bisphenols because this bioanalytical technique has some advantages, such as high selectivity, low production cost, short analytical cycle, simple instrumentation, and easy automation.^[32] However, enzymatic biosensors mostly suffer from low stability of enzymes. Therefore, other more stable and reliable methods are needed for the determination of bisphenols. Nowadays, MIPs and DNA-aptamers based electrochemical sensors show higher sensitivity and selectivity toward bisphenols comparing to that of the enzyme-based sensors.^[29–31,33] A number of researches were dedicated to the detection of

bisphenol A. However, some improvements in the development of analytical systems dedicated for the determination of bisphenol S are still required. Thus, we are predicting that the formation of MIP-Ppy imprinted by bisphenol S formed over the network of 1D ZnO nanostructures eventually can improve the performance of sensor devoted for the determination of bisphenol S.

The aim of this research was to develop photoelectrochemical sensor based on ZnO-NRs/MIP-Ppy structure devoted for selective determination of bisphenol S.

2. Experimental Section

2.1. Materials

Zinc acetate dehydrate, hexamethylenetetramine, 2-propanol (IPA), ethanolamine, sodium sulphate, and zinc nitrate hexahydrate were obtained from Sigma-Aldrich (Riga, Latvia), and were used without additional purification. The conducting glass fluorine doped tin oxide (FTO) (8 mm × 25 mm) were cleaned by successive sonication with deionized water and isopropyl alcohol for 10 min, with rigorous drying prior to further procedures, and then it was subjected to plasma treatment for 15 min in order to eliminate all traces of organic materials.

2.2. Synthesis of ZnO-Nanorods

ZnO-nanorods were deposited by hydro-thermochemical method. Initial ZnO seed layer has been prepared on FTO-glass by drop casting of 20 μL of 1 mg mL^{-1} zinc acetate methanol solution, followed by annealing at 350 °C for 1 h. The FTO substrates with ZnO seed layers were for 2 h incubated in 50 mM of zinc nitrate and 50 mM of hexamethylenetetramine containing solution in water at 90 °C. A hydrothermal growth of ZnO-NRs was performed. The samples were washed by deionized water and then dried at room temperature.

2.3. Electrochemical Deposition of Polypyrrole

Cyclic voltammetry (CV) was used for the modification and characterization of FTO/ZnO-NRs-based electrodes using Autolab potentiostat/galvanostat (model PGSTAT 100, Ecochemie B.V., Utrecht, The Netherlands). Pt foil, Ag/AgCl and FTO/ZnO-NRs were used as a counter electrode, a reference electrode and a working electrode, respectively. Ten potential cycles in the range of 0–0.9 V versus Ag/AgCl at sweep rate of 100 mV s^{-1} were performed for the deposition of MIP-Ppy on FTO/ZnO-NRs electrode in 0.1 M PBS solution, containing 10 mM of bisphenol S (BPS) and 1 mM of pyrrole monomer. The BPS molecules were removed by continuous overoxidation of Ppy, which was involved in the formation of FTO/ZnO-NRs/MIP-Ppy structure, in 0.1 M sodium sulphate (Na_2SO_4) at fixed potential of +0.9 V versus Ag/AgCl applied for 10 min.

The electrochemical analysis of FTO/ZnO-NRs/MIP-Ppy electrodes was performed in 0.1 M phosphate buffer solution

(PBS). The home-made UV light source with the intensity of 4 mW at 365 nm was used to excite the working electrode.

2.4. Structural and Optical Characterization

Structural properties of the FTO/ZnO-NRs/MIP-Ppy electrode were investigated by SEM (Zeiss Evo HD15 SEM from Zeiss Ltd (Jena, Germany)) and FTIR (FTIR-ATR spectrophotometer "Frontier" from Perkin Elmer (Waltham, USA)) spectroscopy. Optical properties were studied by reflectance spectroscopy using HR2000+ fiber spectrometer from Ocean Optics (Dunedin, USA).

2.5. Determination of Analytical Characteristics

The ZnO-NRs/MIP-Ppy samples were incubated in bisphenol S solution in PBS. After 5 min of incubation the electrochemical determination of analytical signal was performed. The electrochemical determination of bisphenol S was based on applying sequence of multiple potential pulses and measurement of peak current during these pulses, as it was described in earlier researches of the authors.^[10,34] The applied voltage profile of potential pulses was: 20 s at +0.0 V versus Ag/AgCl and 20 s at +0.5 V versus Ag/AgCl, a sequence of 5 such pulses was applied for each measurement performed by potentiostat/galvanostat.

In order to perform control measurements, a non-imprinted polypyrrole (NIP-Ppy) was deposited over FTO/ZnO-NRs electrode (FTO/ZnO-NRs/NIP-Ppy). All conditions for the formation of NIP-Ppy were kept the same excluding the presence of bisphenol S molecules in polymerization bulk solution. In addition, sensitivity and selectivity of FTO/ZnO-NRs/MIP-Ppy and FTO/ZnO-NRs/NIP-Ppy electrodes toward bisphenol C (as a compound, which is very similar to analyte—bisphenol S) was tested.

3. Results and Discussion

SEM images of ZnO-nanorods before and after the deposition of MIP-Ppy are shown in **Figure 1a,b**, respectively. As deposited ZnO-NRs were of 30 ± 15 nm in diameter and of 800 ± 40 nm in length (Figure 1a). MIP-Ppy deposition over ZnO-NRs formed a shell of MIP-Ppy on the surface of FTO/ZnO-NRs (grey and black areas in Figure 1A). The composition of the ZnO-NRs/MIP-Ppy nanocomposite has been verified by FTIR measurements (**Figure 2a,b**). As deposited ZnO-nanorods have shown two optical absorption shoulders at 400 and 600 cm^{-1} , which correspond to ZnO vibrational modes.^[35] Formed ZnO-NRs/MIP-Ppy nanocomposite showed several new peaks at 1049, 1249, 1379, 1591, 2885, 2980 and 3423 cm^{-1} , which are corresponding to Ppy, formed over ZnO-NRs. Bare Ppy has absorption peaks at 792 (C–H wagging), 912 (plane ring deformation), 1044 (=C–H– in plane vibration), 1120 (C–H stretching), 1204 (C–N stretching), 1289 (C–C stretching), 1409 (C–N stretching in benzoyl ring), 1556 (C=C stretching in benzoyl ring), 1719 (C=N), 2852 (stretching CH₂), 2926 (anti-symmetric stretching CH₂), and 3115–3300 cm^{-1}

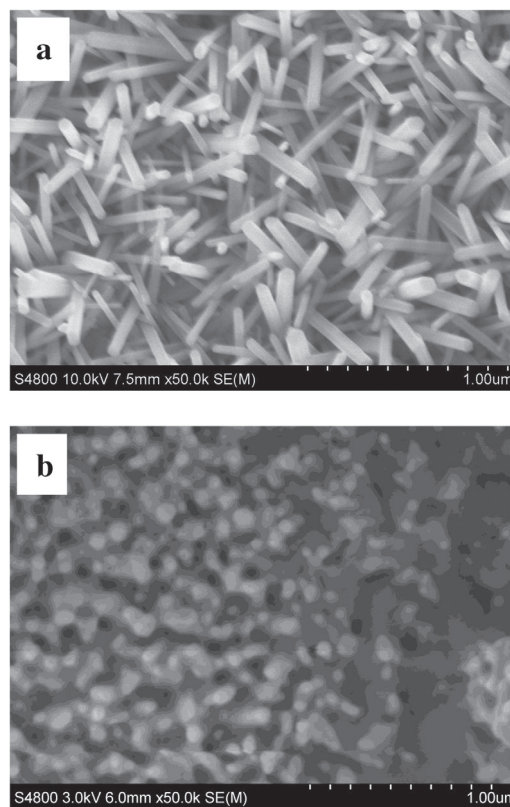


Figure 1. SEM images of a) FTO/ZnO-NRs- and b) FTO/ZnO-NRs/MIP-Ppy-based electrodes.

(N–H stretching).^[6–8] According to results, reported in other researches,^[6–8] the quenching and shifting of FTIR peaks of Ppy after the electrochemical deposition on ZnO point to forming of nanocomposite. In other researches has been supposed that hydrogen bonds are formed between oxygen of ZnO-nanorod-structure and hydrogen involved in N–H groups of Ppy.^[6–8]

Reflectance measurements of FTO/ZnO-NRs and FTO/ZnO-NRs/MIP-Ppy electrode surfaces showed significant change of reflectance and blue-shift of absorption edge of ZnO-NRs

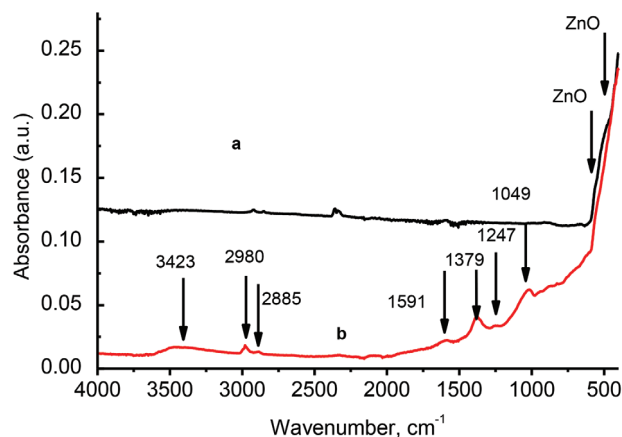


Figure 2. FTIR spectra of a) FTO/ZnO-NRs- and b) FTO/ZnO-NRs/MIP-Ppy-based electrodes.

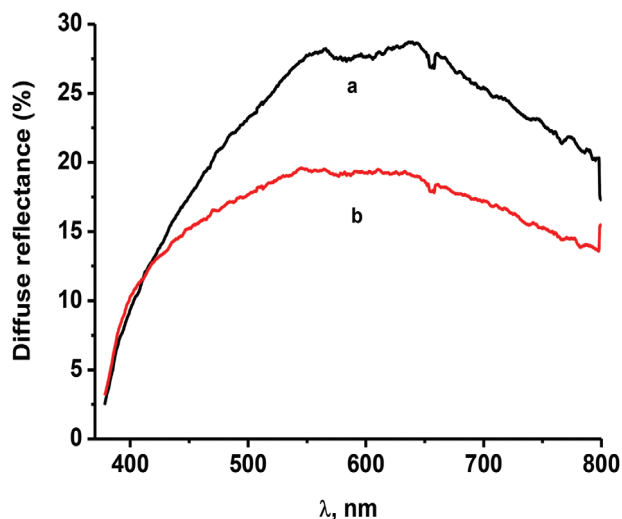


Figure 3. Diffuse reflectance of a) FTO/ZnO-NRs- and b) FTO/ZnO-NRs/MIP-Ppy-based electrodes.

after MIP-Ppy deposition (Figure 3a,b). The band gaps, which were calculated according to methodology presented in other research, were 3.16 and 3.22 eV for ZnO-NRs and ZnO-NRs/MIP-Ppy, respectively.^[36]

Summarized data of cyclic voltammetry (CV) are shown in Figure 4. FTO/ZnO-NRs electrode showed significant increase of current, induced by UV light excitation (Figure 4, curve b) comparing to the current observed during measurements in the absence of illumination (in the “dark”) (Figure 4, curve a). The increase of photoinduced current is related to significant increase of charge-carrier concentration due to photo-generated electron-hole pairs. However, the current value does not increase if applied voltage is in the range of -0.7–0 V versus Ag/AgCl, pointing out that the main charge carriers in

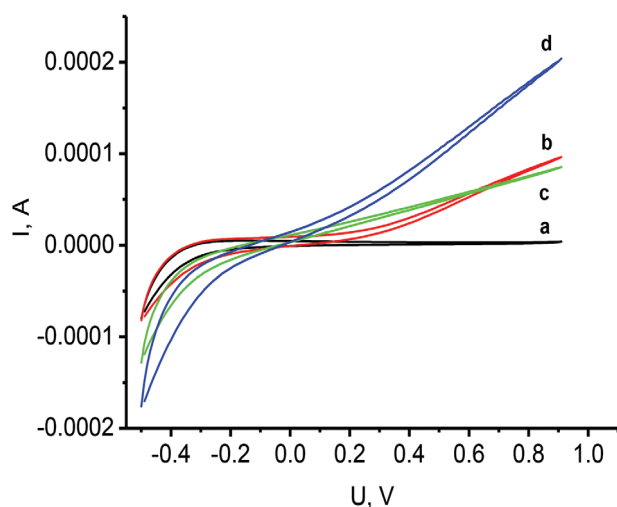


Figure 4. Cyclic voltammograms of FTO/ZnO-NRs- and FTO/ZnO-NRs/MIP-Ppy-based electrodes: a) FTO/ZnO-NRs-based electrode at “dark” conditions, b) FTO/ZnO-NRs-based electrode under UV excitation, c) FTO/ZnO-NRs/MIP-Ppy-based electrode at “dark” conditions, d) FTO/ZnO-NRs/MIP-Ppy-based electrode under UV excitation.

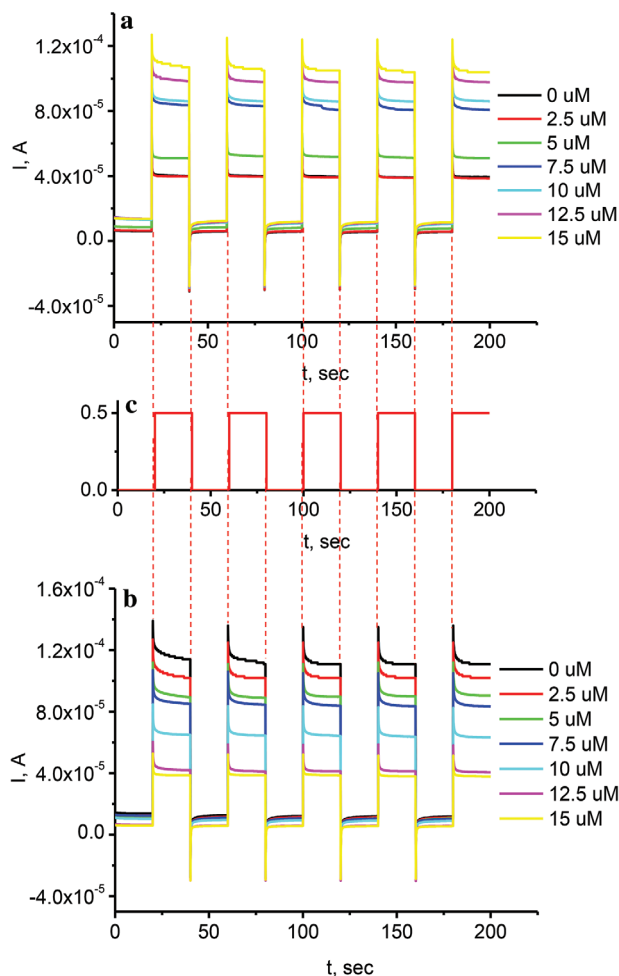


Figure 5. Chrono amperometric response of FTO/ZnO-NRs/MIP-Ppy-based electrode toward bisphenol S: a) at “dark” conditions; b) at UV excitation; c) potential pulse profile, which was applied for the determination of electro-analytical signal.

FTO/ZnO-NRs-modified electrode are electrons. The current value in FTO/ZnO-NRs/MIP-Ppy electrodes has significantly increased in comparison to that of FTO/ZnO-NRs electrode (Figure 4, curve c and Figure 4, curve d). The increase of the current under negative potentials points to increased hole concentration after the deposition of MIP-Ppy layer. Ppy is typically p-type semiconductor, therefore the formation of p-n junction has been expected between ZnO-NRs and Ppy in FTO/ZnO-NRs/MIP-Ppy-based electrode.^[17,19,37]

Amperometric response of FTO/ZnO-NRs/MIP-Ppy electrode to bisphenol S (BPS) is shown in Figures 5a,b. It was determined, that the current of FTO/ZnO-NRs/MIP-Ppy electrode increased after incubation in bisphenol S containing solution at “dark” conditions and it decreased under UV excitation. The sensor signal was calculated according to equation:

$$S_{(C)} = I_{(UV)} - I_{(dark)} \quad (1)$$

In addition, control measurements of FTO/ZnO-NRs (Figure S1, Supporting Information) and FTO/ZnO-NRs/MIP-Ppy

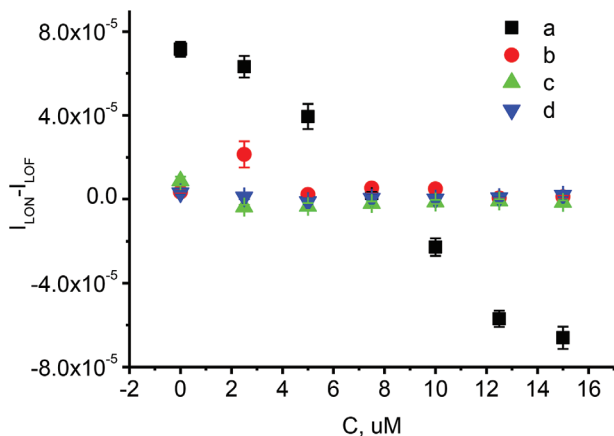


Figure 6. Photo-electrochemical response of a) FTO/ZnO-NRs/MIP-Ppy-based electrode toward bisphenol S, b) FTO/ZnO-NRs/NIP-Ppy-based electrode toward bisphenol S, c) FTO/ZnO-NRs-based electrode toward bisphenol S, d) FTO/ZnO-NRs/MIP-Ppy-based electrode toward bisphenol C.

(Figure S2, Supporting Information) electrodes toward bisphenol were performed at i) “dark” conditions and ii) under UV excitation. Selectivity test of FTO/ZnO-NRs/MIP-Ppy to bisphenol C was studied (Figure S3, Supporting Information) at conditions described above.

The principal differences between FTO/ZnO-NRs/MIP-Ppy and FTO/ZnO-NRs/NIP-Ppy electrodes are as follows:

At “dark” conditions registered current increased for both FTO/ZnO-NRs/MIP-Ppy (Figure 5A) and FTO/ZnO-NRs/NIP-Ppy (Figure S2A, Supporting Information) electrodes when bisphenol S was added;

At UV excitation signal increased for FTO/ZnO-NRs/NIP-Ppy (Figure S2B, Supporting Information) electrode and decreased for FTO/ZnO-NRs/MIP-Ppy (Figure 5B) electrode when bisphenol S was added;

The sensor signal, calculated as a difference between the signal registered at UV excitation and at “dark” conditions do not show significant dependence on bisphenol S concentration in the case of FTO/ZnO-NRs/NIP-Ppy electrode. The difference in action of MIP-Ppy- and NIP-Ppy-based electrodes was that at UV excitation signal for FTO/ZnO-NRs/NIP-Ppy electrode decreased compared (Figure S2B) to that at “dark” conditions (Figure S2A), while for FTO/ZnO-NRs/NIP-Ppy electrode the effect was opposite (Figure 5). It allows us to predict that some photochemical processes occur between FTO/ZnO-NRs/Ppy and bisphenol S in the case of FTO/ZnO-NRs/MIP-Ppy-based electrode when bisphenol S is filling within Ppy imprinted cavities.

FTO/ZnO-NRs/MIP-Ppy-based sensor responses are summarized in **Figure 6**. It is clearly seen that FTO/ZnO-NRs/MIP-Ppy-based sensor showed good sensitivity to bisphenol S. The sensor showed selectivity toward other bisphenol compounds (**Figure 7**).

The sensor signal ($B_{(C)}$) was calculated in the following way:

$$B_{(C)} = (S_{(0)} - S_{(C)})/S_{(0)} \quad (2)$$

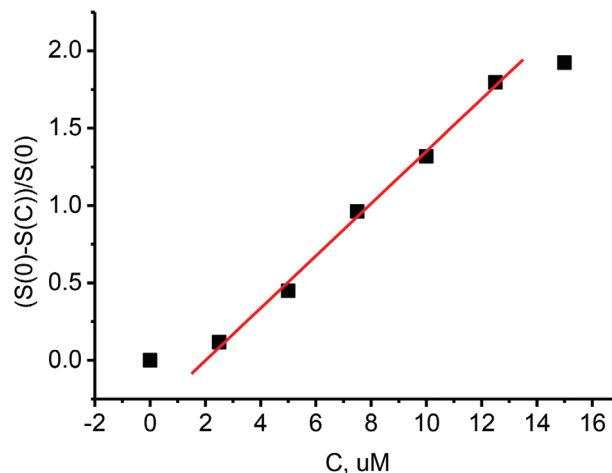


Figure 7. Sensitivity of FTO/ZnO-NRs/Ppy-MIP-based electrode to bisphenol S.

where $S_{(0)}$ and $S_{(C)}$ are sensor signals at $0 \mu\text{M}$ and at applied concentration (C) μM of bisphenol S, respectively.

Linear response was observed in the range of 2.5–12.5 μM of bisphenol S. Limit of the detection of FTO/ZnO-NRs/MIP-Ppy-based electrode was calculated as:

$$\text{LOD} = 3 \sigma / b \quad (3)$$

where σ and b are standard deviation of the sensor signal and linear slope value (Figure 6), respectively. The obtained LOD value for bisphenol S was $0.7 \mu\text{M}$.

The reported values of sensitivity to bisphenols of other reported MIP-based sensors are in the range of 0.1–100 μM .^[29,30,33] The sensitivity value depends on the type of MIP and the substrate, on which the MIP layer is formed. Therefore, the sensitivity values toward bisphenol S of FTO/ZnO-NRs/MIP-Ppy electrodes fulfil detection range required for the determination of bisphenol in real samples. Due to high resistance of the ZnO-NRs we suppose, that sensitivity can be increased by the doping of ZnO-NRs with Al or other dopants, which are able to act as electron-donors and to reduce Ohmic resistance of ZnO-NRs-based layer and in such way to increase the registered current.

4. Conclusion

Novel photo-electrochemical sensor based on FTO/ZnO-NRs/MIP-Ppy has been developed. The sensor was sensitive toward bisphenol S. The proposed sensor showed higher sensitivity under UV excitation, compared to that when measurements were performed at “dark” conditions. The FTO/ZnO-NRs/MIP-Ppy photo-electrochemical sensor showed sensitivity to bisphenol S in the range of 2.5–12.5 μM with the limit of detection of $0.7 \mu\text{M}$. The developed MIP-Ppy layer showed good selectivity toward bisphenol S compared to some other bisphenolic compounds, such as bisphenol C.

Supporting Information

Supporting Information is available from the Wiley Online Library or from the author.

Acknowledgements

D.E. and R.V. acknowledge financial support from Taiwan -Latvia -Lithuania Cooperation Project LV -LT -TW/2019/1, and R.V., A.R., D.E. and A.R. acknowledge financial support from the European Union's Horizon 2020 MSCA-RISE-2017 project CanBioSe under grant agreement no. 778157.

Conflict of Interest

The authors declare no conflict of interest.

Keywords

bisphenol, molecularly imprinted polymers, photoelectrochemical sensors, photoinduced, photoluminescence

Received: May 29, 2019
Revised: September 1, 2019
Published online:

- [1] A. Tereshchenko, M. Bechelany, R. Viter, V. Khranovsky, V. Smytyna, N. Starodub, R. Yakimova, *Sens. Actuators, B* **2016**, 229, 664.
- [2] G. Manasa, R. J. Mascarenhas, A. K. Satpati, B. M. Basavaraja, S. Kumar, *Colloids Surf., B* **2018**, 170, 144.
- [3] R. Viter, M. Savchuk, I. Iatsunskyi, Z. Pietralik, N. Starodub, N. Shpyrka, A. Ramanaviciene, A. Ramanavicius, *Biosens. Bioelectron.* **2018**, 99, 237.
- [4] C. Paladiya, A. Kiani, *Sens. Actuators, B* **2018**, 268, 494.
- [5] V. Manthina, A. G. Agrios, *Nano-Struct. Nano-Objects* **2016**, 7, 1.
- [6] A. Pruna, Q. Shao, M. Kamruzzaman, Y. Y. Li, J. A. Zapien, D. Pullini, D. Busquets Mataix, A. Ruotolo, *Appl. Surf. Sci.* **2017**, 392, 801.
- [7] S. Jain, N. Karmakar, A. Shah, D. C. Kothari, S. Mishra, N. G. Shimpi, *Appl. Surf. Sci.* **2017**, 396, 1317.
- [8] A. Pruna, Q. Shao, M. Kamruzzaman, J. A. Zapien, A. Ruotolo, *Electrochim. Acta* **2016**, 187, 517.
- [9] L. J. Zapata, E. M. Acevedo, in *Advance in Nanotechnology*, Nova publishers, New York **2014**, pp. 221.
- [10] A. Ramanaviciene, A. Ramanavicius, A. Finkelsteinas, *J. Chem. Educ.* **2006**, 83, 1212.
- [11] V. Ratautaite, D. Plausinaitis, I. Baleviciute, L. Mikoliunaite, A. Ramanaviciene, A. Ramanavicius, *Sens. Actuators, B* **2015**, 212, 63.
- [12] I. Baleviciute, V. Ratautaite, A. Ramanaviciene, Z. Balevicius, J. Broeders, D. Croux, M. McDonald, F. Vahidpour, R. Thoelen, W. De Ceuninck, K. Haenen, M. Nesladek, A. Reza, A. Ramanavicius, *Synth. Met.* **2015**, 209, 206.
- [13] V. Ratautaite, S. D. Janssens, K. Haenen, M. Nesladek, A. Ramanaviciene, I. Baleviciute, A. Ramanavicius, *Electrochim. Acta* **2014**, 130, 361.
- [14] V. Ratautaite, M. Nesladek, A. Ramanaviciene, I. Baleviciute, A. Ramanavicius, *Electroanalysis* **2014**, 26, 2458.
- [15] V. Ratautaite, S. N. Topkaya, L. Mikoliunaite, M. Ozsoz, Y. Oztekin, A. Ramanaviciene, A. Ramanavicius, *Electroanalysis* **2013**, 25, 1169.
- [16] A. Ramanaviciene, A. Ramanavicius, *Biosens. Bioelectron.* **2004**, 20, 1076.
- [17] A. Batool, F. Kanwal, M. Imran, T. Jamil, S. A. Siddiqi, *Synth. Met.* **2012**, 161, 2753.
- [18] M. A. Chougule, S. Sen, V. B. Patil, *Synth. Met.* **2012**, 162, 1598.
- [19] M. A. Chougule, D. S. Dalavi, S. Mali, P. S. Patil, A. V. Moholkar, G. L. Agawane, J. H. Kim, S. Sen, V. B. Patil, *Measurement* **2012**, 45, 1989.
- [20] E. S. Kwak, A. Just, R. Whyatt, R. L. Miller, *Open Allergy J.* **2009**, 2, 45.
- [21] B. O. Opeolu, O. S. Fatoki, J. Odendaal, *Int. J. Environ. Anal. Chem.* **2010**, 5, 576.
- [22] K. Larsson, K. Ljung Björklund, B. Palm, M. Wennberg, L. Kaj, C. H. Lindh, B. A. G. Jönsson, M. Berglund, *Environ. Int.* **2014**, 73, 323.
- [23] L. Robinson, R. Miller, *Curr. Environ. Health Rep.* **2015**, 2, 379.
- [24] P. Reboredo-Rodríguez, E. Valli, A. Bendini, G. Di Lecce, J. Simal-Gándara, T. Gallina Toschi, *Eur. J. Lipid Sci. Technol.* **2016**, 118, 1593.
- [25] A. Azzouz, E. Ballesteros, *J. Chromatogr. A* **2014**, 1360, 248.
- [26] A. Bajoub, S. Medina-Rodríguez, M. Gómez-Romero, E. A. Ajal, M. G. Bagur-González, A. Fernández-Gutiérrez, A. Carrasco-Pancorbo, *Food Chem.* **2017**, 215, 245.
- [27] W. Lu, X. Wang, X. Wu, D. Liu, J. Li, L. Chen, X. Zhang, *J. Chromatogr. A* **2017**, 1483, 30.
- [28] C. C. Mayorga-Martinez, M. Guix, R. E. Madrid, A. Merkoj, *Chem. Commun.* **2012**, 48, 1686.
- [29] F. Tan, L. Cong, X. Li, Q. Zhao, H. Zhao, X. Quan, J. Chen, *Sens. Actuators, B* **2016**, 233, 599.
- [30] W. Zheng, Z. Xiong, H. Li, S. Yu, G. Li, L. Niu, W. Liu, *Sens. Actuators, B* **2018**, 272, 655.
- [31] M. K. Li, L. Y. Hu, C. G. Niu, D. W. Huang, G. M. Zeng, *Sens. Actuators, B* **2018**, 266, 805.
- [32] N. Ben Messaoud, M. E. Ghica, C. Dridi, M. Ben Ali, C. M. A. Brett, *Talanta* **2018**, 184, 388.
- [33] K. Yan, Y. Yang, J. Zhang, *Sens. Actuators, B* **2018**, 259, 394.
- [34] A. Ramanavicius, Y. Oztekin, A. Ramanaviciene, *Sens. Actuators, B* **2014**, 197, 237.
- [35] R. Viter, I. Iatsunskyi, V. Fedorenko, S. Tumenas, Z. Balevicius, A. Ramanavicius, S. Balme, M. Kempinski, G. Nowaczyk, S. Jurga, M. Bechelany, *J. Phys. Chem. C* **2016**, 120, 5124.
- [36] M. Nasr, R. Viter, C. Eid, F. Warmont, R. Habchi, P. Miele, M. Bechelany, *RSC Adv.* **2016**, 6, 103692.
- [37] S. R. Nalage, M. A. Chougule, S. Sen, P. B. Joshi, V. B. Patil, *Thin Solid Films* **2012**, 520, 4835.